G05

Proceedings of the 5th International Conference on Inverse Problems in Engineering: Theory and Practice, Cambridge, UK, 11-15th July 2005

ESTIMATION OF A SOURCE TERM IN A TWO-DIMENSIONAL HEAT TRANSFER PROBLEM: APPLICATION TO AN ELECTRON BEAM WELDING, THEORETICAL AND EXPERIMENTAL VALIDATIONS

J. GUO[1], P. LE MASSON[1], S. ROUQUETTE[2], T. LOULOU[1] and E. ARTIOUKHINE[3].
[1] *LET2E/ETM : Laboratoire d'Etudes Thermique Energétique et Environnement / Equipe Thermophysique et Matériaux. Université de Bretagne Sud, C.U.R.S.T., Rue de Saint Maudé, F-56321 Lorient Cedex, France*
e-mail : jialin.guo@univ-ubs.fr; philippe.le-masson@univ-ubs.fr; tahar.loulou@univ-ubs.fr
[2] *Laboratoire des Systèmes Mécaniques et Ingénierie Simultanée (LASMIS). Université de Technologie de Troyes - FRE CNRS 2719 - 12 Rue Marie Curie - 10010 TROYES Cedex, France*
e-mail : sebastien.rouquette@utt.fr
[3] *Laboratoire CREST, UMR CNRS 6000, Université de Franche-Comté - Université de Technologie de Belfort-Montbéliard, Site IGE, 2 avenue Jean Moulin, 90000 Belfort, France*
e-mail : eugene.artioukhine@univ-fcomte.fr

Abstract - This paper is concerned with the estimation of a heat source applied in the electron beam welding process by using temperature measurements in solid phase. The aim is to identify the energy distribution which is applied in the liquid and vapor zones. This identification is realized each time in a transversal plan perpendicularly to the welding axis. For this work, the goals are, first, to analyze the feasibility of the estimation and, second, to estimate the energy distribution in a real case. The thermometallurgical model does not take into account the convective phenomena in the fused zone. Finally, the iterative regularization method is used for the two-dimensional metallurgical inverse heat transfer problem.

NOMENCLATURE

a	thermal diffusivity ($m^2.s^{-1}$)
b	constant of the austenite - martensite transformation
C_p, C_γ, C_α	specific heat ($J.\ kg^{-1}.\ K^{-1}$)
D^n	vector of descent direction
dT/dt	variation of the temperature with time ($K.s^{-1}$)
$f\left(\partial T / \partial t\right)$	Function of the cooling or warming speed
$\Delta Fo = \frac{a\,\Delta t}{(\Delta x)^2}$	delta Fourier number
h	penetration (m)
H	enthalpy ($J.m^{-3}$)
ΔH_{fus}, ΔH_{vap}	enthalpies of the phase change ($J.kg^{-1}$)
I, I_f	current and focus current (A)
J(S)	residual functional
∇J^n	the gradient of the residual functional
$L_{\alpha\gamma}$	heat transformation of phase α to γ ($J.m^{-3}$)
M_s	martensite start temperature
n, n*	iteration number, last iteration
P, P_{eq}	proportion of metallurgic phase (per volume fraction)
P_{max}	maximum proportion of the austenite phase during the austenite – martensite transformation
P_α, P_γ	proportion of the ferrite and austenite phase
S^{n+1}, S(x,z,t)	source term
T_{inf}	external temperature (°C).
T, T_0	temperature in the sample and initial temperature in the sample (°C)
t	time coordinate (s)
U	voltage (V)
V	velocity (m/s)
x, y, z	spatial coordinates (m)
Y, Y_i, Y_e	experimental temperatures (°C)
γ^n	descent parameter
δ^2	convergence criterion

ε	emissivity of the sample
ε_1	arrest criterion
η	efficiency coefficient
λ, λ_α, λ_γ	conductivity ($W.m^{-1}.K^{-1}$)
ρ, ρ_α, ρ_γ	density ($kg.m^{-3}$)
σ	Boltzmann constant : $5.67\ 10^{-8}\ Wm^{-2}K^{-4}$
σ^2	standard deviation of the temperature measurement errors
τ	time constant
$\theta(z,r,t)$	temperature variation
Φ	beam diameter (m)
$\Psi(z,r,t)$	adjoint variable

1. INTRODUCTION

Welding is an assembling operation which affects both mechanical and structural properties and which is very sensitive to control parameters of technological processes. The first stage of this study is to choose those parameters which lead to an acceptable welding quality. The main difficulty of the theoretical analysis is that the exact distribution of the thermal energy absorbed and generated in the liquid and vapor zones is not easy to predict and cannot be measured directly. When studying the welding, the theoretical analysis use complementary experimental information: the temperature measurements near the liquid zone and the microstructural properties (hardness, optical micrograph...). The objective of this work is the estimation of the energy distribution in the welding zone. The temperature difference between the welding and solid zones is big enough, but there is a strong damping effect in the solid zone. That is why it is difficult to estimate correctly the energy distribution from the temperature measurements taken at points which are too far from the welding zone. Many works deal with the estimation of boundary conditions or the determination of distributed heat flux on the boundary of the body [1-3]. Few of these works consider experimental situations involving unknown heat sources. Silva Neto and Ozisik [4] used the conjugate gradient algorithm to estimate the time-varying strength of a line source placed in a rectangular region with insulated boundaries, but the location of the source was specified. Le Niliot [5] studied linear inverse problems with two point heat sources, and experimental results were presented in [6].

In many studies, the inverse fusion and solidification problem has been analyzed using a simplified approach based on only a conduction model in the liquid and vapor zones. Under these assumptions, 1D or 2D Stefan problems taking into account only the conduction effects in all the phases during the process were considered. The objective was to estimate an energy distribution [3], or a motion of the solid-liquid interface [7-10]. Another approach was to take into account the convection effects describing the Navier-Stokes equations in the liquid and vapor zones [11]. At last, mixed approaches were employed, in which an apparent source term is determined in the liquid and vapor zones representing the different phenomena [12].

In this paper, we use the first hypothesis for the electron beam welding process. We consider only the conduction effects for all phases (solid, liquid and vapor). The iterative regularization method [2] is used to estimate the dissipation energy in the liquid and vapor zones. First, we present the electron beam welding technique and the used steel sample. Second, we describe the direct problem including the simulation of phase transformations and the source term (electron beam). Third, the estimation procedure is described. Fourth, the feasibility of the estimation is analysed. Finally, the experimentation and the estimation results are discussed.

2. THE ELECTRON BEAM WELDING

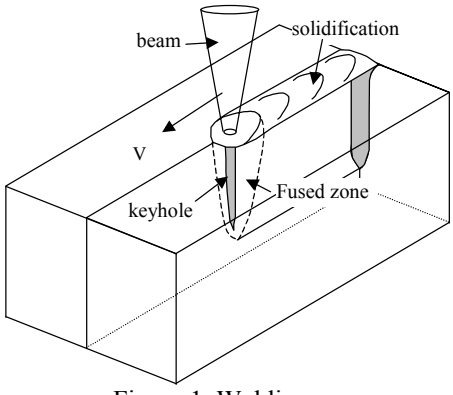

Figure 1. Welding process.

2.1 Principle

The electron beam (EB) welding is an assembling process in vacuum using a high density energy beam. This technique permits the welding of high thicknesses (up to 16 cm) with a low width and a narrow Heat Affected Zone (HAZ). At the beginning of the welding process, the high power density of the EB leads to an evaporation of the material and then to a keyhole (Figure 1). It is this keyhole and its displacement which generate the welded joint. The high penetration capacity of the beam with a narrow fusion zone characterizes the EB welding in comparison with other weld methods. For these other methods, the penetration is limited by the heat conduction [13].

For this study, weld joints are used which are realised in the "Direction des Constructions Navales" (DCN) in Indret (44-France) (power of this EB: 100KW). The welds are made of 18MnNiMo 5 steel samples (ASTM A508 Cl.3). In this paper, a partial penetration welded joint is analysed. Figure 2 shows the micrography of this sample which is used to determine precisely the locations of the measurement points by using a scan of this welding joint. The welding parameters are: voltage: U=60kV, current I = 0.29A, velocity v = 2.5mm/s, focus current I_f=2.46A.

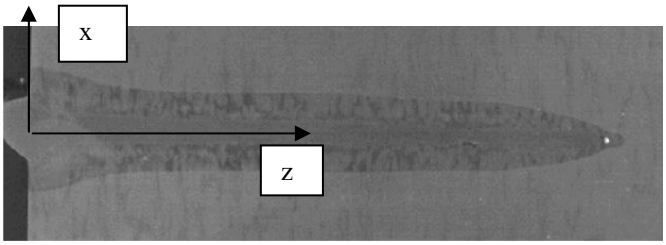

Figure 2. Weld joint.

2.2 Numerical simulation of the electron beam welding

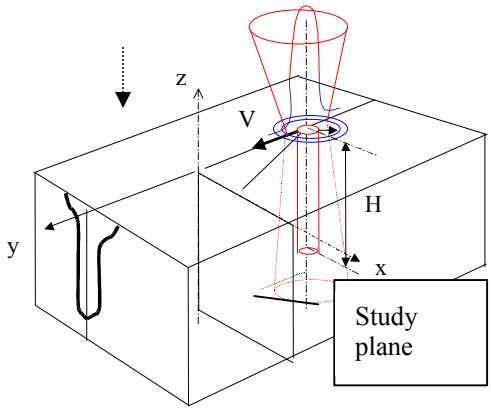

Figure 3. Definition of the study plane.

Several works are concerned with the numerical simulation of the EB welding in the laboratory LET2E [14-16]. In these works, the SYSWELD code [17] was used. In this study, we use a new code analogous to SYSWELD which is incorporated in the developed estimation code. The finite difference method based on an implicit scheme is used to solve the direct and inverse problems. The equations are the heat conduction eqn. (1) and the metallurgical kinetic eqns (2) of the type Leblond and Devaux [18] and Koistinen and Marburger [19]. The studied domain is one half of the transversal plane taken perpendicularly to the welding axis (Figure 3).

$$\rho(T)C_p(T)\frac{\partial T}{\partial t}=\frac{\partial}{\partial x}\left(\lambda(T)\frac{\partial T}{\partial x}\right)+\frac{\partial}{\partial z}\left(\lambda(T)\frac{\partial T}{\partial z}\right)+\frac{\partial P_\alpha}{\partial t}L_{\alpha\gamma}(T)-\frac{\partial(\rho H)}{\partial t}+S(x,z,t) \quad (1)$$

$$\frac{\partial P}{\partial t}=\frac{P_{eq}-P}{\tau}f\left(\frac{\partial T}{\partial t}\right) \text{ and } P=P_{max}\left(1-exp\left(-b\left(T-M_s\right)\right)\right) \quad (2)$$

The boundary and initial conditions are the following: at the lower, upper and lateral surfaces, only the radiative conditions are fixed because the welding process is carried out in a vacuum. For example, at the lower surface, the boundary condition is:

$$-\lambda(T)\frac{\partial T(x,z=0,t)}{\partial z}=\varepsilon\sigma\left[T^4(x,z=0,t)-T_{inf}{}^4\right] \quad (3)$$

On the axis: $$\frac{\partial T(x=0,z,t)}{\partial x} = 0 \quad (4)$$

Initial conditions: $$T(x, z, 0) = T_0 \;\; ; \;\; P_\alpha (x, z, 0) = 1 \quad (5)$$

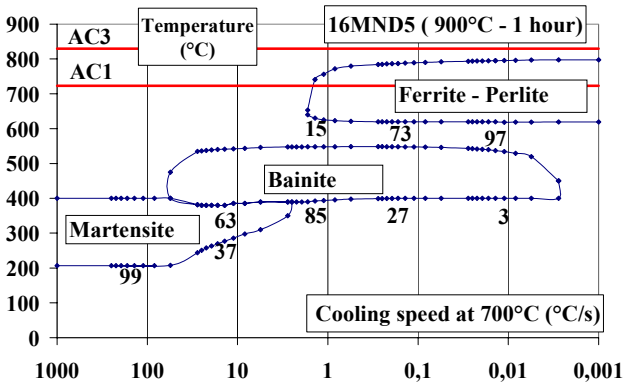

Figure 4. CCT diagram.

In the heat conduction eqn. (1), the source terms $\frac{\partial P_\alpha}{\partial t} L_{\alpha\gamma}(T)$ and $\frac{\partial(\rho H)}{\partial t}$ take into account the phase change enthalpy according to the temperature of the sample (metallurgical transformations for the first term - P_α is the proportion of metallurgic phase α, fusion and evaporation for the second). The transformation energy is calculated according to the phase enthalpy: $L_{\alpha\gamma}(T) = \rho_\gamma H_\gamma - \rho_\alpha H_\alpha$ and by considering two metallurgical phases only: γ (austenite) and α (ferrite, perlite, bainite or martensite). The enthalpies of the phases α and γ are computed with the use of polynomial functions between 100 °C and 1450 °C. The parameters of the metallurgical kinetic equations are calculated by simulating the CCT diagram (Figure 4).

For each time and space node, the cooling speed and the temperature value are used. With this information, the percentage P_i of the metallurgical transformation is computed. Moreover, the thermophysical characteristics $\rho(T), C(T)$ and $\lambda(T)$ are calculated at all time steps by a law of mixtures according to the temperature, e.g. $\lambda(T)=P_\gamma * \lambda_\gamma(T) + P_\alpha * \lambda_\alpha(T) = \sum_i P_i \lambda_i(T)$.

For the phase γ and for T < 1450°C:

$\rho_\gamma * C_\gamma(T) = 3641440 + 4638.78*T - 11.7784*T^2 + 0.0155136*T^3 - 9.29165E\text{-}6*T^4 + 2.03093E\text{-}9*T^5$

$\lambda_\gamma(T) = 0.0148939 + 1.24115E\text{-}5*T - 7.74533E\text{-}10*T^2 + 8.11438E\text{-}13*T^3$

For the phase α and for T < 750°C:

$\rho_\alpha * C_\alpha(T) = 3620850 + 2955.1*T - 7.52398*T^2 + 0.0249182*T^3 - 1.68686E\text{-}5*T^4$

$\lambda_\alpha(T) = 0.0525037 - 3.35115E\text{-}5*T + 1.76665E\text{-}8*T^2 - 1.74307E\text{-}11*T^3$

The other thermal transformations are computed between 1450°C and 1550°C for the fusion and between 2600°C and 2800°C for the evaporation. These enthalpies are given in Costantini [13]: $\Delta H_{fus} = 391970\ J/kg$ and $\Delta H_{vap} = 6332879\ J/kg$. Finally, the thermophysical characteristics of the liquid and vapor phases are computed at the temperature 1450°C.

The initial data of the model is:

-the mesh;

-the thermophysical characteristics $\rho(T), C(T)$, $\lambda(T)$ and $L_{\alpha\gamma}$ for the different phases according to the temperature;

-the initial and final temperatures of thermal transformations for all phases (CCT diagram);

-the initial temperature $T_0 = 20$ °C in whole domain;

-the ambient temperature T_{inf};

-the emissivity of the considered material is supposed to be constant and equal to 0.8.

The set of equations is solved with the use of a fine discretization of the domain near the EB zone (176 nodes in the vertical direction; 52 nodes in the transverse direction). The finite difference grid is uniform in the vertical direction, $\Delta z = 0.5$ mm, and non-uniform in the transverse direction, $0.05\text{mm} < \Delta x < 2$ mm. The direct problem and the corresponding code have been verified in previous papers [14-16].

Figure 5 shows the comparison between the experimental data and numerical results for a Gaussian source [14]. Globally, we find a good level for the maximal temperatures. Some problems remain because we do not have the diffusion effect forward of the beam. For this reason, it seems to be important to estimate an apparent source term for modeling the diffusion effect in the steel.

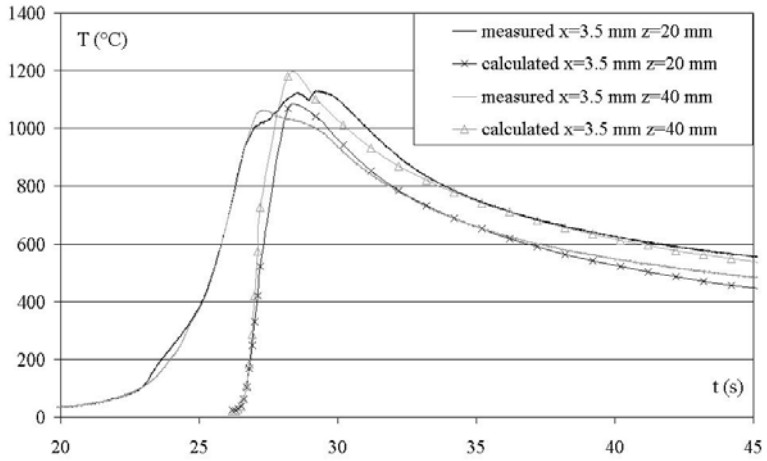

Figure 5. Comparison between the experimental and numerical temperatures.

3. ESTIMATION ALGORITHM

The objective of this research is to determine a source term S(x,z,t). The determination is conducted from the temperature values measured in the heat affected zone at a distance between 2 mm and 8 mm from the welding axis. The time step used in the estimation is $\Delta t = 0.01s$ and the discretization on the welding axis is $\Delta z = 0.5mm$ and $\Delta x = 0.05mm$.

3.1 Minimization procedure

The use of the iterative regularization method leads to the variational formulation of the inverse problem of estimating the source term and the residual functional minimization by utilizing the unconstrained conjugate gradient method. The residual functional is defined as:

$$J(S) = \frac{1}{2} \int_0^{t_f} \sum_{j=1}^{N} \left[T(x_j, z_j, t; S) - Y_j(t) \right]^2 dt \tag{6}$$

where $T(x_j, z_j, t; S)$ and $Y_j(t)$ are the computed and measured temperature histories, respectively, at N various measurement points of the material. The inverse algorithm consists in minimizing this residual functional under constraints on the temperature given by the direct problem (eqns (1)-(5)).

The function S(z,x,t) is considered as an element of the Hilbert space L^2. The source term is computed as a grid function. In the iterative method, the desired function approximations are built at each iteration as follows:

$$S^{n+1} = S^n + \gamma^n D^n, \qquad n=1,\ldots,n^* \tag{7}$$

where n is the iteration index, n* is the index of the last iteration, γ^n is the descent parameter, D^n is the descent direction given by:

$$D^n = -\nabla J^n + \beta^n D^{n-1} \tag{8}$$

$$\text{where: } \beta^n = \frac{\left\langle \nabla J^n - \nabla J^{n-1}, \nabla J^n \right\rangle}{\left(\nabla J^n \right)^2}, \ \beta^0 = 0. \tag{9}$$

$\langle , \rangle$ is the scalar product in Hilbert space L^2, S^0 is an initial approximation of the function to be estimated given *a priori*.

In the absence of noise, the iteration procedure is carried on until the following stopping criterion is verified:

$$\left|\frac{S^{n+1}-S^{n}}{S^{n}}\right| \leq \varepsilon_1 \tag{10}$$

The residual functional gradient ∇J^n is calculated at each computational grid node (x, z, t) by the following analytical relationship:

$$\nabla \mathrm{J}^{\mathrm{n}} = \Psi(\mathrm{x}, \mathrm{z}, \mathrm{t}) \tag{11}$$

where Ψ(x,z,t) is the solution of the adjoint problem [14] derived by using the approach given in [2]. The descent parameter of γ^n is computed as follows:

$$\gamma^{n} = -\frac{\sum_{j=1}^{N}\int_{0}^{t_f}\left[T(x_j,z_j,t)-Y_j(t)\right]\theta(x_j,z_j,t)\,dt}{\sum_{j=1}^{N}\int_{0}^{t_f}\theta^2(x_j,z_j,t)\,dt} \tag{12}$$

where $\theta(x,z,t)$ is the solution of the direct problem in variations [14].

The three systems (direct, in variation and adjoint) are solved numerically using a finite difference method and an implicit scheme.

3.2 Regularization

The inverse problems are ill-posed and numerical solutions depend on the fluctuations occurring at the measurements. Small fluctuations at the measurements can generate big errors in the inverse problem solution. So regularization is needed to stabilize the solution. According to the iterative regularization method, the regularizing discrepancy criterion is used for the stabilization:

$$\mathrm{J}(\mathrm{S}) \cong \delta^2 \tag{13}$$

$$\text{where } \delta^2 = \int_0^{t_f}\sum_{j=1}^{N}\sigma^2\left(x_j,z_j,t\right)dt \tag{14}$$

$\sigma^2(x_j,z_j,t)$ is the standard deviation of the temperature measurement errors. The index n* is the regularization parameter in the method.

4. NUMERICAL SIMULATION

To verify the numerical algorithm, two test cases with exact forms of the source term given *a priori* are analyzed. The results of these theoretical estimations are shown in the previous works [14, 20]. Here, we present only the results for the second form, a Gaussian source which corresponds to several studies carried out in the laboratory LET2E [14, 15]:

$$S(x,z,t) = \frac{8\eta U I_b}{\pi\Phi^2}\exp\left(-\frac{8\left(x^2+(Vt-y_s)^2\right)}{\Phi^2}\right) f(z,h) \quad \text{with} \quad f(z,h) = \frac{2}{h}\left(1-\frac{z}{h}\right) \tag{15}$$

where the parameters are : efficiency coefficient η=0.9, voltage: U=60kV, current: I_b = 0.29A, velocity: V = 2.5mm/s, penetration: h=7.1cm, beam diameter: Φ=0.6 mm.

The Gaussian source is divided in two parts. The first one S_v (most energetic part) (Figure 6 and Figure 7) is applied in the domain where it goes inside the material (creation of the keyhole). The second one S_s (a ring shape – Figure 6) is only a surface heat source corresponding to the "non active" part of the beam. In this paper, we deal only with the estimation of the most energetic part. With these distributions, we can obtain simulated fused and heat affected zones close enough to those shown in Figure 2 [14].

Here, we use, for the estimation, only the exact measurements computed in the HAZ during 0.5s. This time corresponds to the crossing of the analyzed plane by the beam (0<t<0.35s) and the beginning of the cooling. Figure 8 shows three computed temperature histories taken in the HAZ. The maximum temperature is around 1400°C. On the welding axis the maximum calculated temperature is around 6000°C, which demonstrates the high damping in the material. In this case, the Fourier number is calculated with average values: a=5 10^{-6} m²/s, Δx=1.5mm, Δt=0.001s and it is equal to ΔFo=0.002.

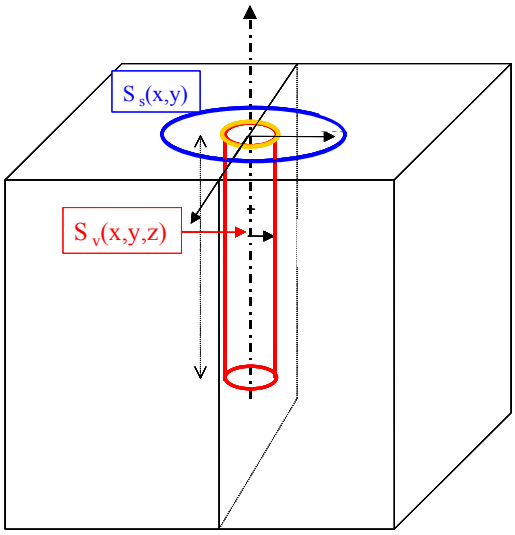

Figure 6. Source definition.

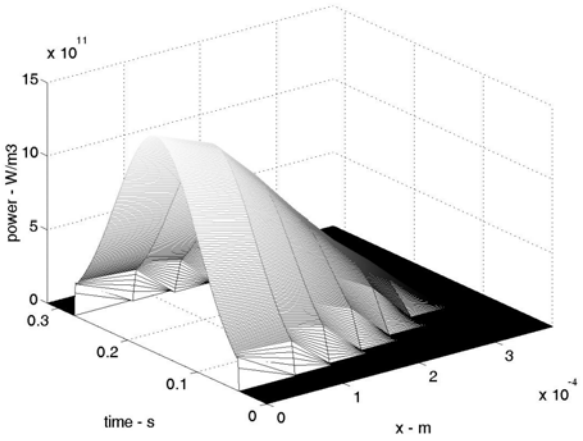

Figure 7. Exact Gaussian source at z=0.

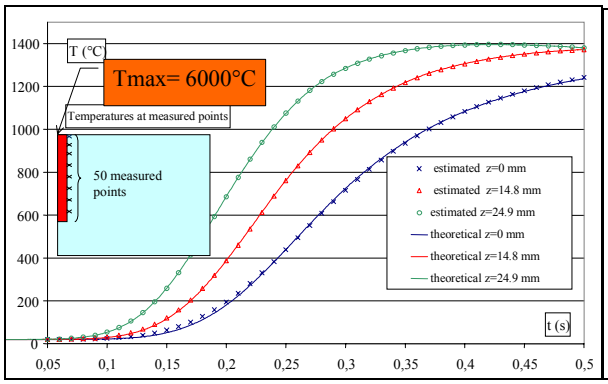

Figure 8. Comparison of the temperatures.

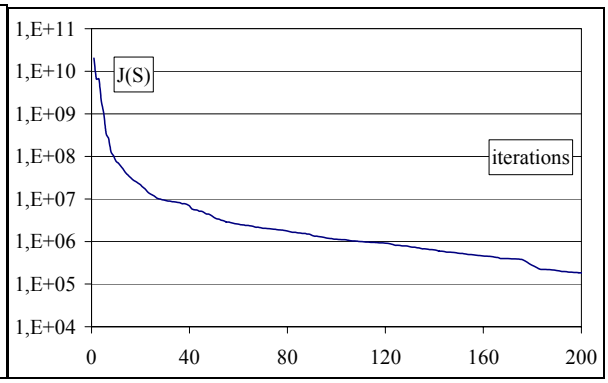

Figure 9. The residual functional evolution.

The analysis of the estimation results (Figure 8 – Figure 11) permits the underscoring of the following points. If we compare the exact and estimated temperatures, it can be seen that the results are good enough. But after 200 iterations (Figure 9), we do not correctly find the Gaussian shape of the source term in transversal direction (Figure 10). Globally, we find the average values of the source. On the other hand, the Gaussian form, as a function of time, is correct. An analysis of this mean heat distribution depending on the depth shows that the estimated form follows well the exact function $f(z,h) = \frac{2}{h}\left(1-\frac{z}{h}\right)$.

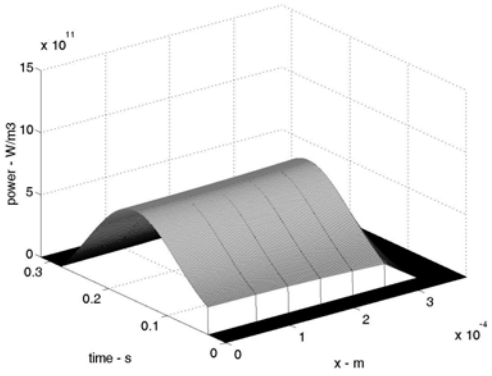

Figure 10. Estimated source at z=0.

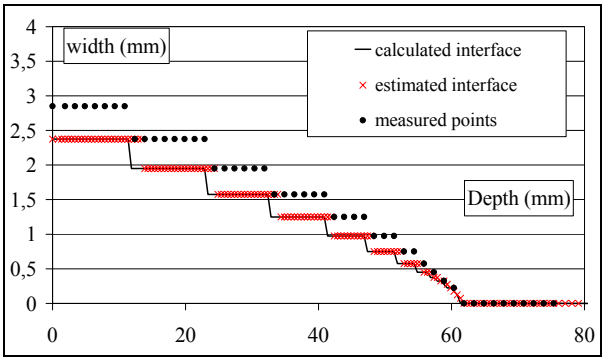

Figure 11. Evolution of the fused zone.

Another comparison point is the boundary of the fusion zone. Figure 11 shows these exact and estimated boundaries. In the scale of the computational finite difference grid, the shape is followed well. Finally, one can see that it is more difficult to obtain the convergence to the exact source term for the beginning of the welding process. This difficulty comes from the fact that there is no conduction effect forward the beam (only a transversal plan is analyzed). So, the temperature variation is very abrupt when the beam arrives at the study plan. In reality, the thermocouples give information on the beam due to the conduction effects and it is easier to estimate the source term at the beginning of the welding process.

5. APPLICATION

5.1 The experiment

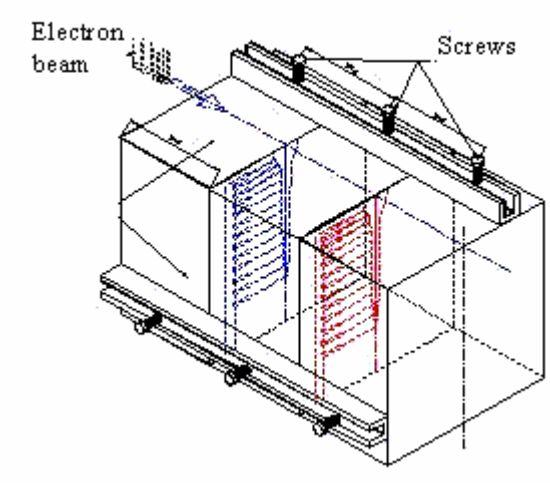

Figure 12. First block.

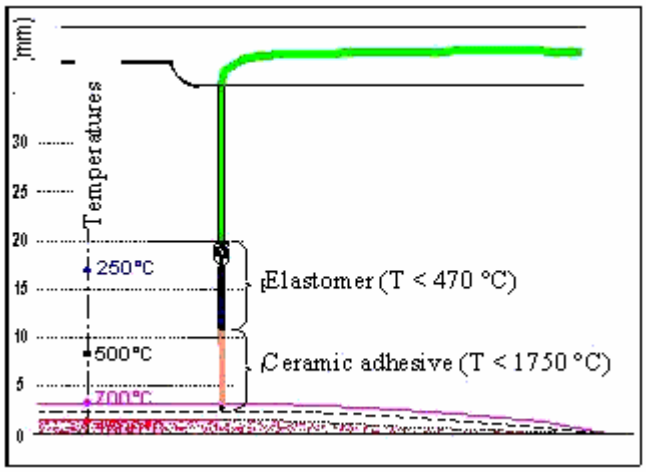

Figure 13. Thermocouple installation.

The numerical estimation of the source term (test cases) by different methods [14] has shown that it is difficult to obtain the space distribution of energy in each plane perpendicular to the welding axis. On the other hand, the distribution of energy according to the depth as well as the relative position of the source with respect to this depth remain potentially identifiable. The presented experimental work was carried out in the laboratory LET2E since 2000 [21]. This led us to propose a method of thermocouple installation based on the cutting of the samples in order to carry out a fine instrumentation inside the samples [14, 21]. Figures 12 and 13 present the principle of cutting of the samples as well as the thermocouple installation (type K - 50µm). Two blocks (figure 12) were equipped with 93 thermocouples, distributed on four interfaces. These sensors were located mainly in the heat affected zones. Each thermocouple is welded by capacitive discharge at the bottom of a small hole (diameter 400 µm, depth 500 µm). The wires of 50 µm diameter are then brought out thanks to grooves obtained by electroerosion to a basin (with approximately 20mm of the axis of welding) where a connection with wires of 125 µm is carried out. The wires are then protected and insulated electrically by a high temperature adhesive (Aremco Ceramabond 571 - Tmax = 1750°C) and by an elastomer (T < 470°C). After the thermocouple installation, the recombining of the blocks (figure 2) is obtained by fastening to some welding points. The EB welding experiment was developed on the industrial site of the DCN establishment. The EB welding machine has a power of 100 KW with a vacuum chamber volume of 800 m^3. A "ARATA" type test [22] was carried out on a strip of stainless iron to ensure the reproducibility of the beam form with the shooting reference parameters of welding (U = 60 kV, I_b = 0,29 A, I_f = 2.46 A, V = 2.5 mm /s, distance of shooting = 160 mm). Indeed, the geometry of the beam can change according to the installation ageing. Lastly, the frequency of acquisition is chosen to be 100 Hz over a total recording time of 5 minutes. With different samples, we have collected 93 thermal cycles, 52 thermocouples gave very clean recordings which can be used directly in the estimation code, 28 thermocouples gave truncated information and 13 thermocouples exceeded the acceptable temperature range given by a K type sensor. The last stage of this experimental work consists in an accurate check of the thermocouple locations which is essential to estimate accurately the source term [14].

5.2 The estimation

The estimation of the source term is based on 52 temperature profiles obtained on the four interfaces after a temporal retiming. The significant number of the measurement points as a private individual in the vicinity of surface enables us to make some remarks. First of all, calculation was carried out up to 300 iterations. Figure 14 presents the functional evolution during calculation. In a way identical to the theoretical cases [14], it is shown that the decrease is very fast in the first 20 iterations at the time of convergence towards the density of dissipated power. Thereafter, we note a slower variation after a hundred iterations. At this iteration stage, the estimated source evolves very slowly. The forms of source obtained enable us to note that: first, it is impossible to obtain a

correct distribution according to the transverse direction (an average value is obtained), second, the distribution according to time follows a law of the Gaussian type except close to the surface (Figure 16) where it appears a quantity of considerable energy to the back of the beam certainly related to the fused metal rejection. Moreover, in Figure 15, we can note that the distribution of energy is a depth function with first of all an energy zone near to the surface, then an average value on a middle part of the welding and finally an attenuation of the values to the root of the welding. With the exit of the preceding estimates, we decided to correct the source term in the transverse direction and to impose a Gaussian form. Indeed, for lack of constraint, the method of iterative regularization leads to a spreading out of energy in this direction which does not make it possible to obtain the correct limits of the fused and heat affected zones compared to the experiment. Figure 17 presents the new form of source obtained starting from the estimated source of Figure 16.

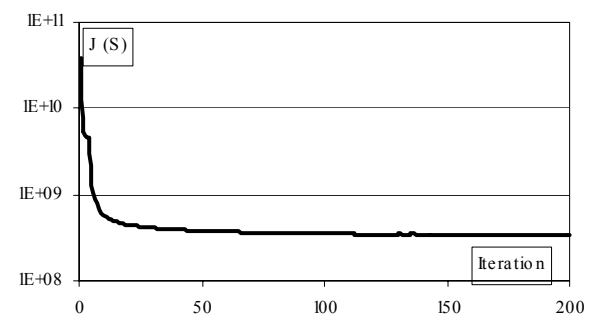

Figure 14. Functional residual.

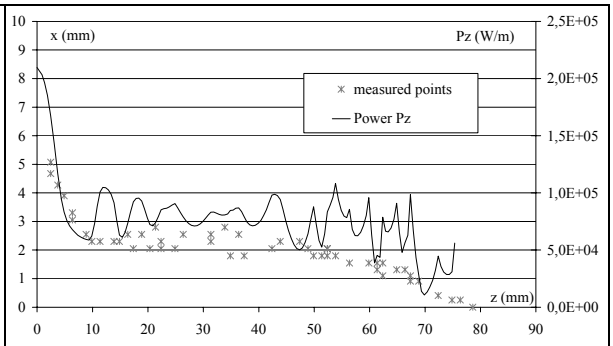

Figure 15. Power density.

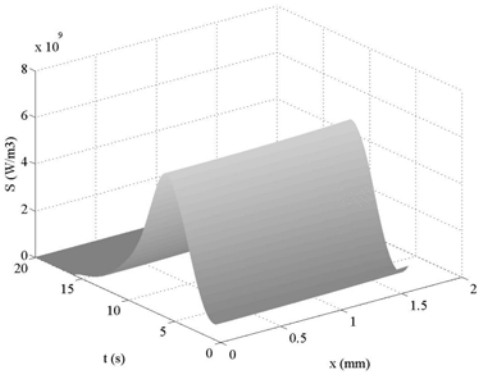

Figure 16. Estimated source at z = 2.47 mm.

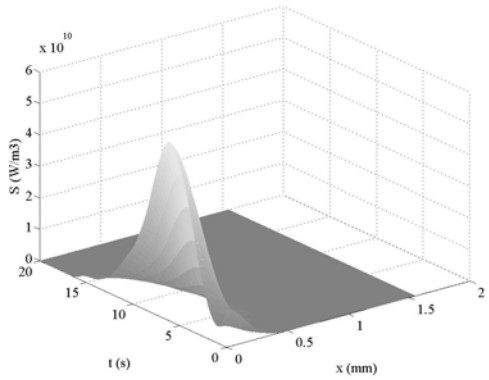

Figure 17. Optimal source at z = 2.47 mm.

6. CONCLUSIONS

The objective of this work was to estimate by the iterative regularization method a source term in the case of the EB welding process. A transient thermometallurgic modelling being based on a transverse plan 2D was carried out. The results show that we have no possibility to correctly describe the energy distribution in the transverse direction. An average and constant value is obtained according to this direction. On the other hand, the distributions according to the direction of welding (y or t) and the depth (z) give us relevant indications. Moreover, the analysis of the energy integral according to depth z shows that the energy distribution is uniform for depths $8 < z < 65$ mm and that it varies at the head and foot of the weld. In the foot of the weld, the power density attenuates while at the head of the weld, the matter rejection accentuates this density. Finally, in order to propose a form of optimal source, and in order to circumvent the difficulty related to the transverse distribution of the energy, we proposed to distribute the average energy estimated in the transverse direction in a Gaussian form. A final analysis of the forms of the fused and heat affected zones shows a difficulty in finding the limit of the fused zone. On the other hand, the limit of the heat affected zone is very well found.

Acknowledgement

The authors acknowledge the CESMAN – DCN Indret for the weld joints.

REFERENCES

1. J.V. Beck, B. Blackwell and C.R. St Clair, *Inverse Heat Conduction. Ill-posed Problems*, Wiley, New York, 1985.
2. O.M. Alifanov, E.A. Artyukhin and S.V. Rumyantsev, *Extreme Methods for Solving Ill-posed Problems with Applications to Inverse Heat Transfer Problems*, Begell House, New York, 1995.
3. Y. Jarny, M.N. Ozisik and J.P. Bardon, A general optimization method using adjoint equation for solving multidimensional inverse heat conduction. *Int. J. Heat Mass Transfer* (1991) **34**, 2911-2919.
4. A.J. Silva Neto and M.N. Ozisik, Two-dimensional inverse heat conduction problem of estimating the time varying strengh of a line source. *J. Appl. Phys.* (1992) **71**, 5357-5362.
5. C. Le Niliot, The boundary element method for the time varying strength estimation of point heat sources: application to a two-dimensional diffusion system. *Numer. Heat Transfer B* (1998) **33**, 301-321.
6. C. Le Niliot and P. Gallet, Infrared thermography applied to the resolution of inverse heat conduction problems : recovery of heat line sources and boundary conditions. *Rev. Gen. Therm.* (1998) **37**, 629-643.
7. S. Peneau, J.P. Humeau and Y. Jarny, Front motion and convective heat flux determination in a phase change process. *Inverse Problems in Eng.* (1996) **4**, 53-91.
8. R. Keanini and N. Desai, Inverse finite element reduced mesh method for predicting multidimensional phase change boundaries and nonlinear solid face heat transfer. *Int. J. Heat Mass Transfer* (1996) **39**, 1039-1049.
9. Y.F. Hsu, B. Rubinsky and K. Mahin, An inverse finite element method for the analysis of stationary arc welding processes. *J. Heat Transfer* (1986) **108**, 734-741.
10. Y. Ruan and N. Zabaras, An inverse finite element technique to determine the change of phase interface location in two dimensional melting problems. *Commun. in Appl. Numer. Meth.* (1991) **7**, 325-338.
11. N. Zabaras, Adjoint methods for inverse free convection problems with application to solidification processes, *Computational Methods for Optimal Design and Control*, (Eds. J. Borggaard, E. Cliff, S. Schreck and J. Burns), Birkhauser, 1998, pp. 391-426.
12. V. A. Karkhin, V.V. Plochikhine and H.W. Bergmann, Solution of inverse heat conduction problem for determining heat input, weld shape, and grain structure during laser welding. *Science and Technology of Welding and Joining* (2002) **7**, 224-231.
13. M. Costantini, *Simulation Numérique du Soudage par Faisceau d'Electrons - Contribution au Développement d'un Modèle Prédictif de l'Apport d'Energie*, Thèse de l'Université Paris 6, 1995.
14. J. Guo, *Estimation de la Distribution Energétique Induite par un Faisceau d'Electrons dans un Matériau Métallique – Application au Cas du Soudage d'un Acier*, Thèse de l'Université de Bretagne Sud, 2005.
15. P. Rogeon, D. Couedel, D. Carron, P. Le Masson and J.J. Quemener, Numerical simulation of electron beam welding of metals : sensitivity study of a predictive model, *Mathematical Modelling of Weld Phenomena*, (Eds. H.Cerjak and H.K.D.H. Bhadeshia), 2001, pp. 913-943.
16. P. Rogeon, D. Carron, P. Le Masson, D. Couedel, J.J. Quemener, P. Bocquet, M. Gauthier and P. Balladon, Numerical simulation of electron beam welding of metals : Influence of prior austenite grain size on HAZ microstructure in a low alloyed steel, *Welding Journal- Research supplement* (to appear).
17. Manuel d'utilisation "sysweld", Systus International, 1994.
18. J. Leblond and J. Devaux, A new kinetic model for anisothermal metallurgical transformations in steels including effect of austenite grain size. *Acta Metallurgica* (1984) **32**, 137-146.
19. D.P. Koistinen and R.E. Marburger, A general equation prescribing the extent of austenite-martensite transformation in pure iron-carbon alloys and plain carbon steels. *Acta Metallurgica* (1959) **7**, 59.
20. J. Guo, P. Le Masson, E. Artioukhine, T. Loulou, P. Rogeon, M. Carin, M. Dumons and J. Costa, Estimation of a source term in a two dimensional heat transfer problem: Application to an electron beam welding, *4th International Conference on Inverse Problems*, Russia, 2003.
21. M. Carin, P. Rogeon, D. Carron, P. Le Masson and D. Couedel, Numerical simulation of electrons beam welding and instrumental technique. *Revue Européenne des Eléments Finis* (2004) **13**, 247-267.
22. Y. Arata, Evaluation of beam characteristics by the ab test method, Plasma, electron and laser beam technology, Metals Park, Ohio/USA, American Society for Metals, 1986, pp. 177-189.